Supporting

Engineering a light-driven cyanine based molecular rotor to enhance the sensitivity towards the viscous medium

Vishal Kachwal[a], Abhilasha Srivastava[b], Sumukh Thakar[b], Maria Zubiria-Ulacia[c], Diplesh Gautam[d], Syamantak Majumder[b], Venkatesh KP[d], David Casanova[c], Rajdeep Chowdhury[b], Nigam Rath[e], Sudeshna Mukherjee[b]*, Pere Alemany[f]*, Inamur Rahaman Laskar[a]*

(a) Department of Chemistry, BITS Pilani, Pilani Campus, Rajasthan, India; (b) Department of Biological Science, BITS Pilani, Pilani Campus, Rajasthan, India; (c) Donostia International Physics Center (DIPC), 20018 Donostia, Euskadi, Spain and Universidad del País Vasco/Euskal Herriko Unibertsitatea (UPV/EHU), 20018, Donostia, Euskadi, Spain (d) Department of Mechanical Engineering, BITS Pilani, Pilani Campus, Rajasthan, India; (e) Department of Chemistry and Biochemistry and the Centre for NanoScience, University of Missouri-St. Louis (f) Department de Ciència de Materials i Química Física and Institut de Química Teòrica i Computacional (IQTCUB), Universität de Barcelona, Barcelona, Spain.

Corresponiding Authors
Email:-
ir_laskar@pilani.bits-pilani.ac.in (Inamur Rahaman Laskar)
sudeshna@pilani.bits-pilani.ac.in (Sudeshna Mukherjee)
p.alemany@ub.edu (Pere Alemany)

Table of contents

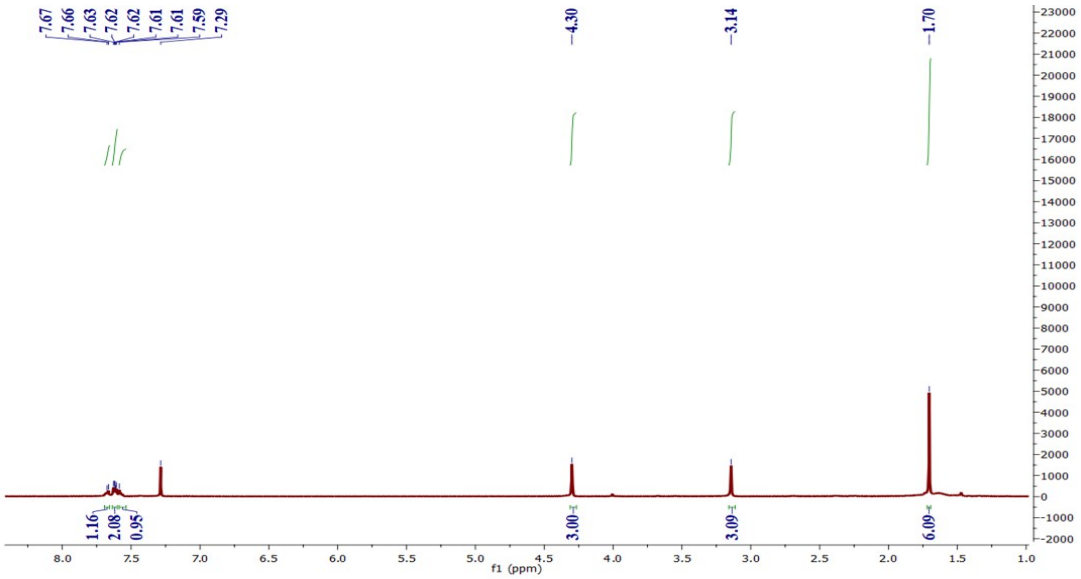

(a) ^{1}H NMR spectrum of L1

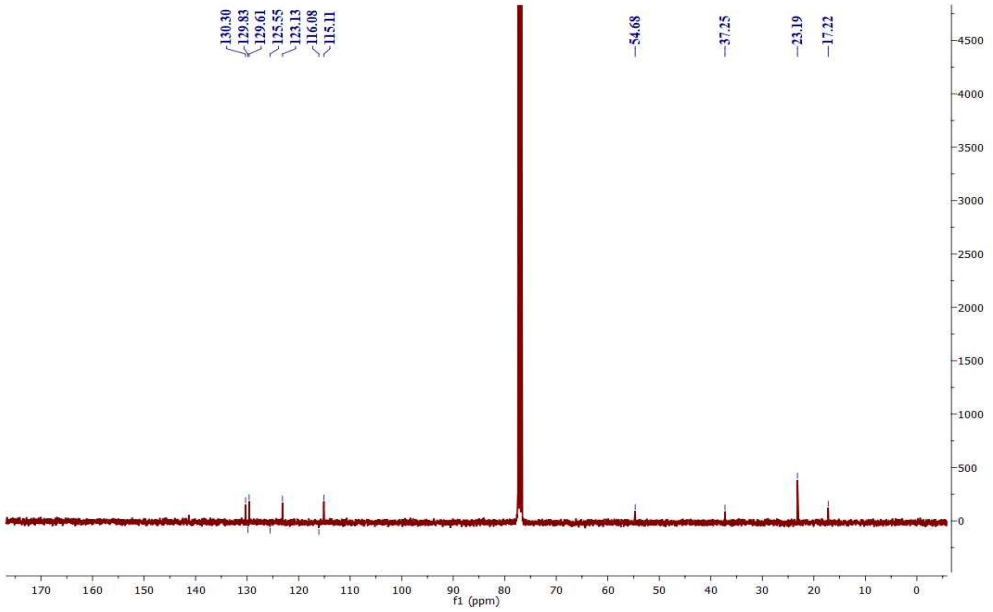

(b) ^{13}C NMR spectrum of L1

Figure S1(a) ^{1}H NMR spectrum of L1 (b)^{13}C NMR Spectrum of L1

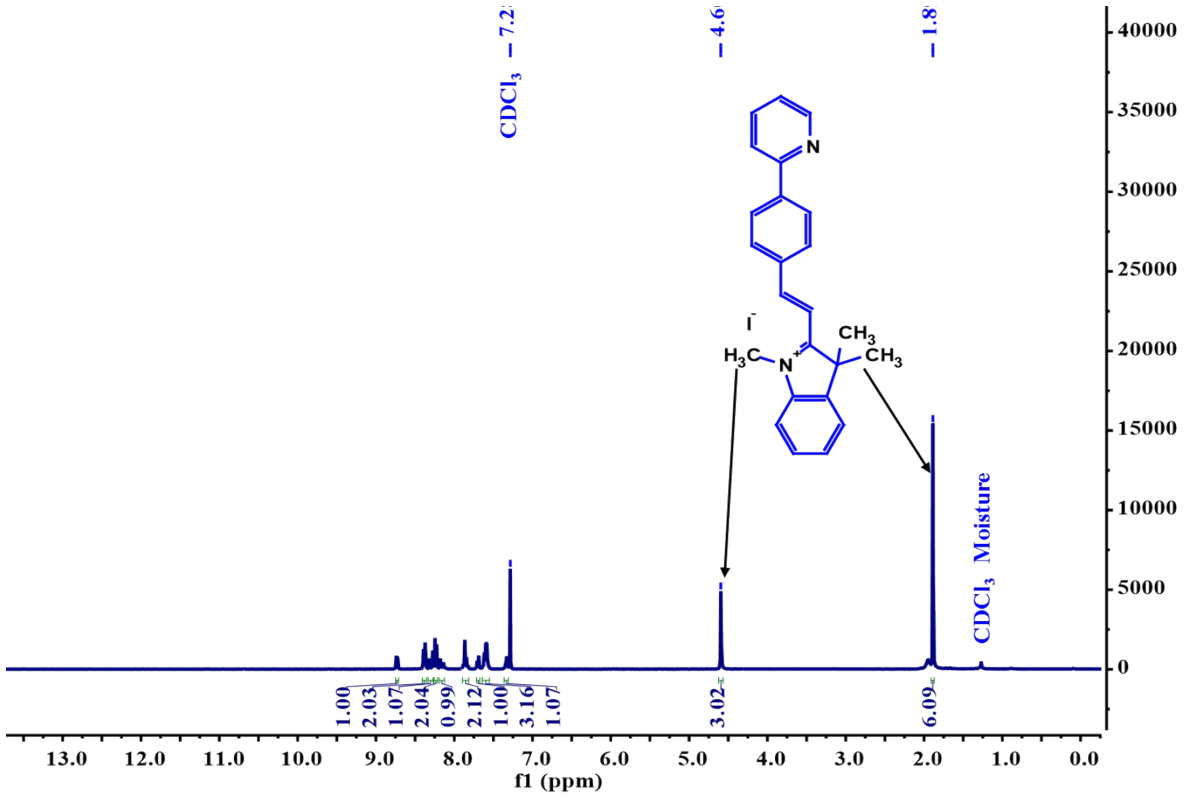

(a)Full Spectrum of ^{1}H NMR spectrum of TPSI I in $CDCl_3$

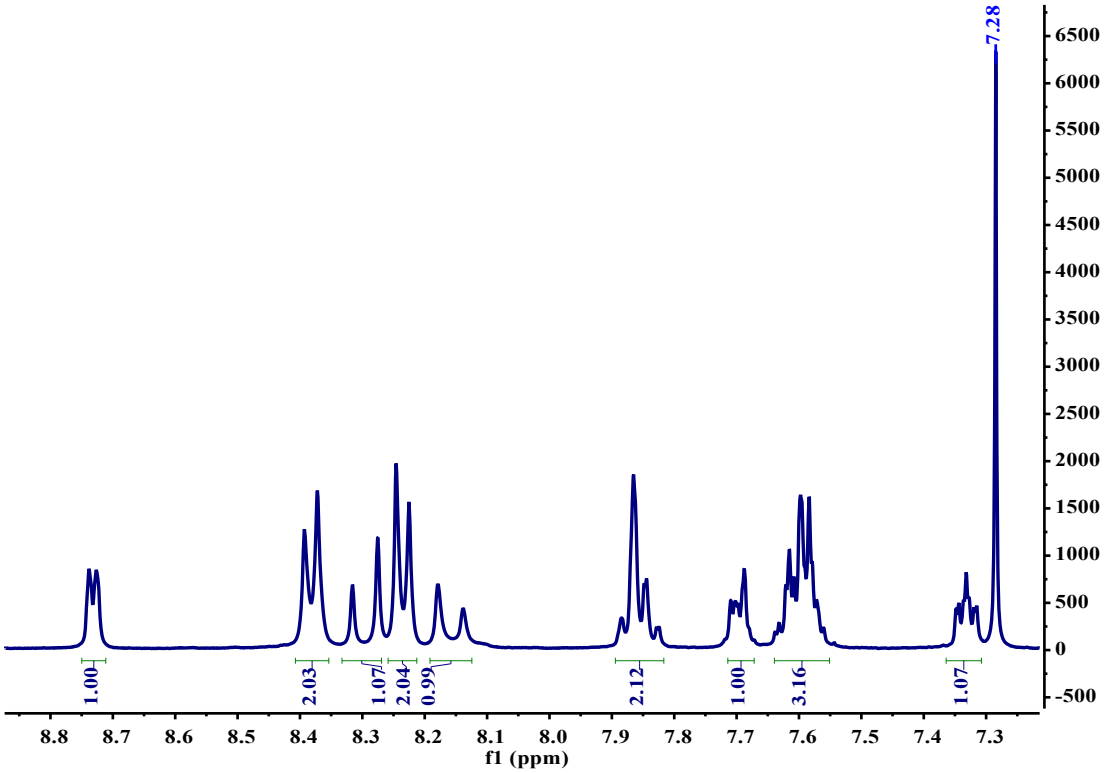

(b) Zoomed part - Aromatic region of the ^{1}H NMR spectrum of TPSI I in $CDCl_3$

^{1}HNMR of TPSI- I δ_H (400 MHz, Chloroform-*d*) 8.74 (1 H, s), 8.38 (2 H, d, *J* 8.3), 8.30 (1 H, d, *J* 16.2), 8.24 (2 H, d, *J* 8.3), 8.16 (1 H, d, *J* 16.2), 7.86 (2 H, d, *J* 6.8), 7.72 – 7.67 (1 H, m), 7.66 – 7.50 (3 H, m), 7.33 (1 H, t, *J* 4.9), 4.60 (3 H, s), 1.89 (6 H, s)

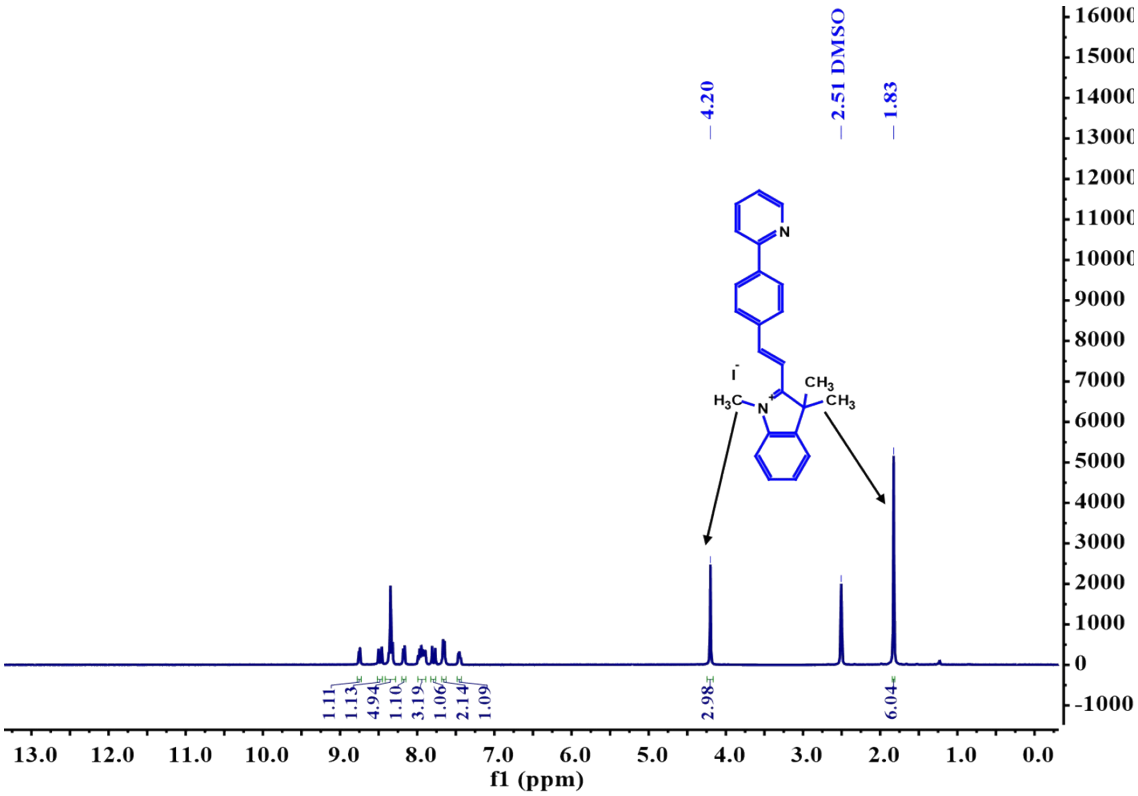

(c)Full Spectrum of ^{1}H NMR spectrum of TPSI I in DMSO

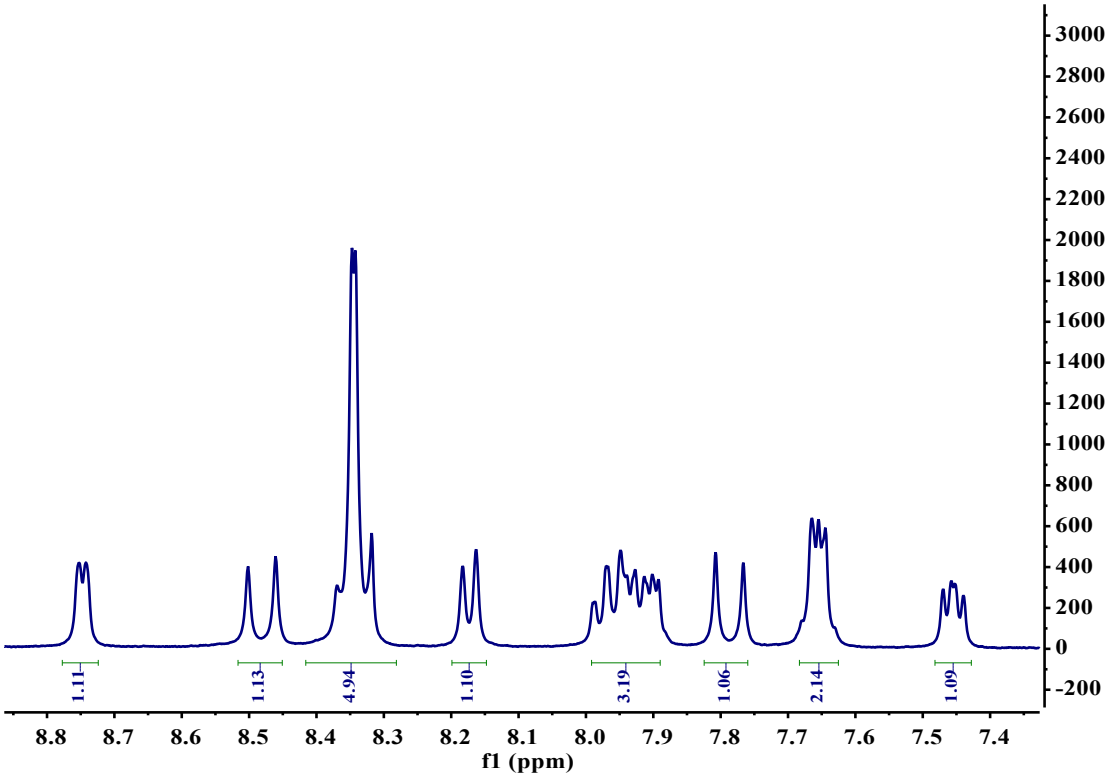

(d)Zoomed part - Aromatic region of the ^{1}H NMR spectrum of TPSI I in DMSO
^{1}H NMR of TPSI I in DMSO δ H (400 MHz, DMSO-d6) 8.75 (1 H, dd, J 4.8, 1.7), 8.48 (1 H, d, J 16.4), 8.42 – 8.28 (5 H, m), 8.17 (1 H, d, J 8.0), 7.99 – 7.89 (3 H, m), 7.79 (1 H, d, J 16.4), 7.68 – 7.63 (2 H, m), 7.45 (1 H, dd, J 7.5, 4.7), 4.20 (3 H, s), 1.83 (6 H, s)

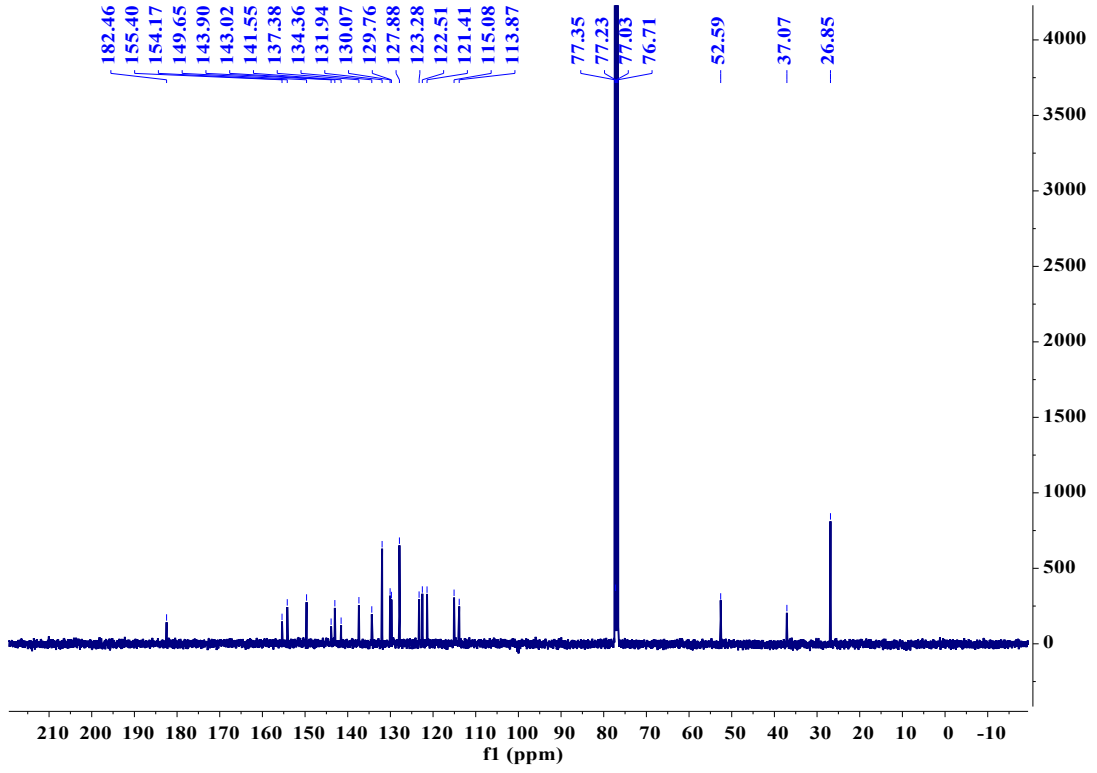

(e) ^{13}C NMR spectrum of TPSI I

^{13}C NMR of TPSI I δ $_C$(101 MHz, $CDCl_3$) 182.46, 155.40, 154.17, 149.65, 143.90, 143.02, 141.55, 137.38, 134.36, 131.94, 130.07, 129.76, 127.88, 123.28, 122.51, 121.41, 115.08, 113.87, 77.35, 52.59, 37.07, 26.85.

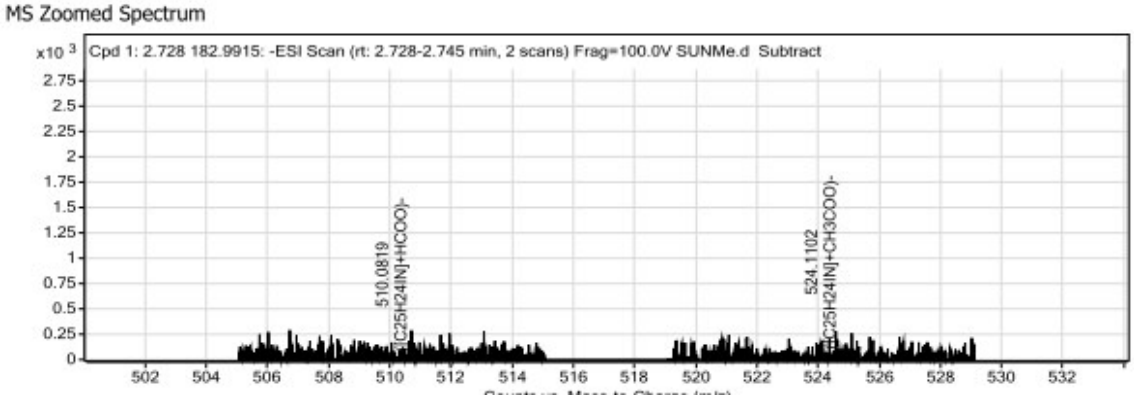

(f)

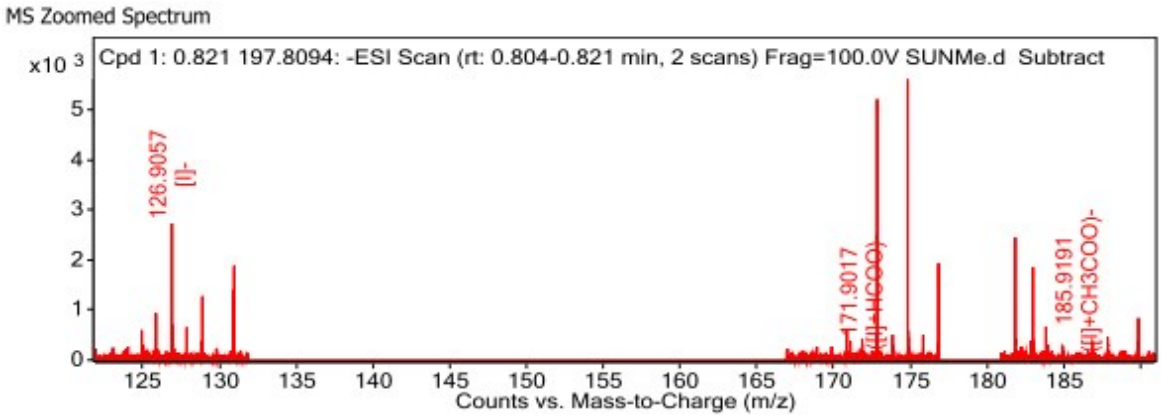

(g)

Figure S2.^{1}H NMR spectra of TPSI I(a, b,) in $CDCl_3$ and (c, d) in DMSO(e) ^{13}C Spectra of TPSI I. HRMS m/z value of (f) TPSI I (g) counter ion (I^-)

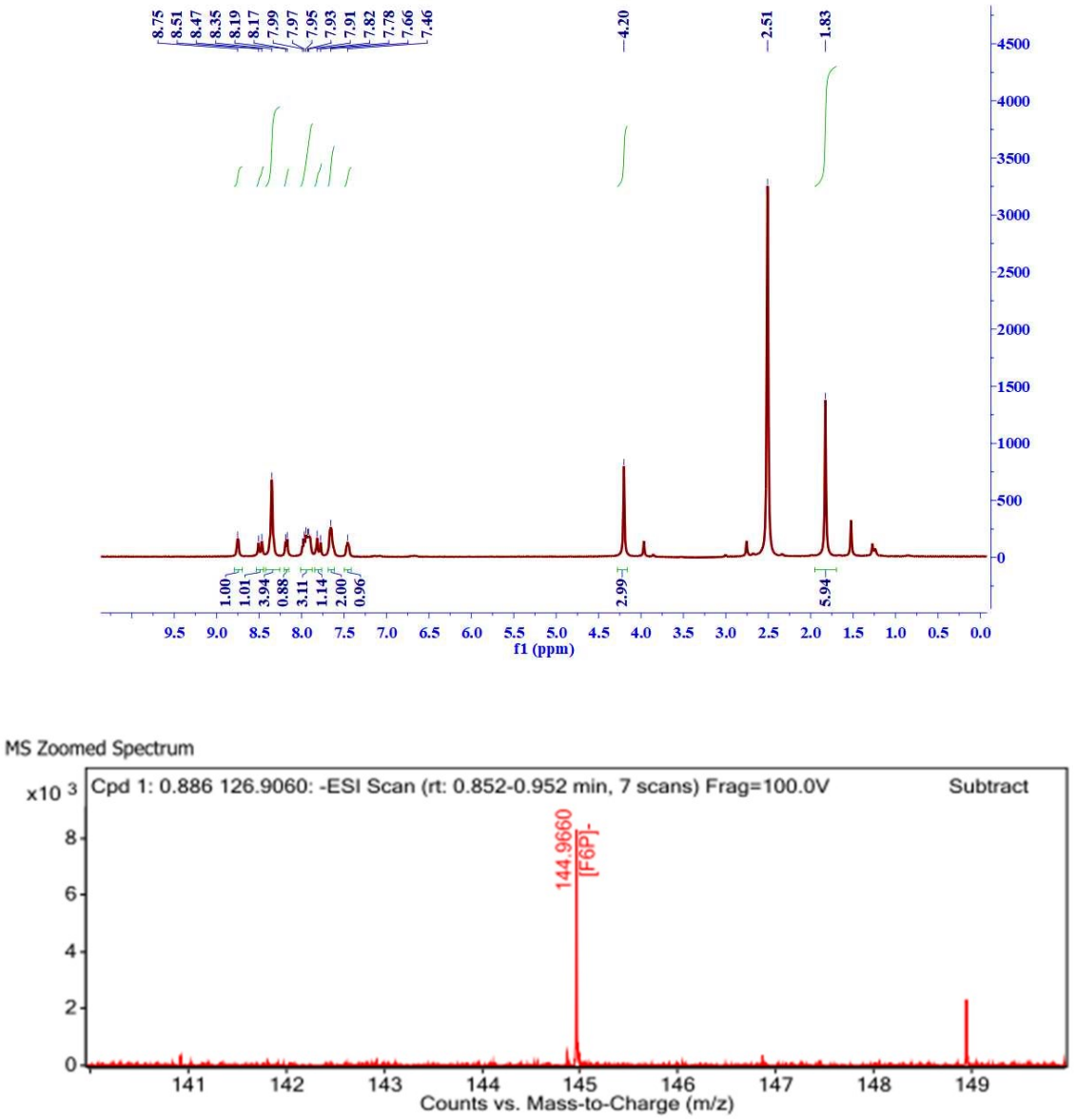

Figure S3. (a) ^{1}H NMR spectrum of TPSI PF_6 in DMSO**(b)**HRMS spectra of TPSI PF_6 Counter ion (PF_6^-)

Cell Culture.

Huh7 (Human hepatocellular carcinoma) were procured from NCCS, Pune, India. Briefly, cells were cultured in Dulbecco's modified eagles' medium (DMEM; Invitrogen) supplemented with 10% fetal bovine serum (FBS; Gibco Life Technologies), 100 UmL^{-1} penicillin and 100μgmL^{-1} streptomycin (Invitrogen) and were maintained at 37° C and 5% CO_2. Cells were grown to 80% confluency before any treatment. Primary culture Human Umbilical Vein Endothelial Cells (HUVEC) were procured from Hi-Media, Bangalore, India and were maintained in iEndoXLTM Endothelial Cell Expansion Medium (HiMedia) containing reduced serum which was then supplemented with endothelial cell growth supplement (HiMedia) and 100 UmL^{-1}

penicillin and 100 μgmL^{-1}streptomycin (Gibco). HUVEC were incubated to maintain the culture at 37° C and 5% CO_2.

Cytotoxicity assay.

In vitro cytotoxicity assay was performed following procedures described earlier by Kovooru et al.[1] Briefly, cells were seeded at a density of 8 × 10^3 in 96 well plates and incubated overnight. The cells were then treated with different doses of either TPSI1 or Methylcellulose (MC) for 24hr. XTT (2,3-bis[2-Methoxy-4-nitro-5-sulfophenyl]-2H-tetrazolium-5-carboxamideinner salt) was added to the treated cells in each well, and cells were incubated for 3hr. Absorbance was measured at wavelength 480nm with a differential filter of 630nm using a Multiskan Microplate Spectrophotometer (Thermo Scientific). The percentage of viable cells was calculated using the formula: Viability (%) = (mean absorbance value of treated cells)/mean absorbance value of control) *100

Microscopic Imaging and Flow Cytometry.

Huh7 cells were seeded on coverslips in a 6-well plate. To modulate intra-cellular viscosity, cells were treated with methyl cellulose (MC) for 24 h. The probe TPSI I was added 2 h prior to harvesting of cells. In studies performed using primary culture, Human Umbilical Vein Endothelial Cells (HUVECs) were grown on gelatin-coated cover glasses for overnight, followed by treating the cells with 30 mM of glucose for 24 h. Treated HUVECs were then incubated with the probe compound for 4 hr. Next, the medium was removed, cells were rinsed in 0.1M phosphate buffer saline (PBS) solution and then fixed using methanol at -20°C for 10 min. The coverslips from both the normal and tumor cell cultures were mounted with an anti-fade mountant (Thermo Scientific) on a glass slide and visualized under a fluorescence microscope (Zeiss Axio Scope A1). For flow cytometry, cells were grown in 6-well plates and were exposed to MC. The probe TPSI I was added 2 h before harvesting the cells for analysis. The cells were then collected and suspended in PBS followed by acquisition using a flow cytometer (CytoFlex, Beckmann Coulter). A shift in fluorescence in the green filter was monitored and the data was analyzed using CytExpert.

Table S1.

Crystal data and structure refinement for TPSI I

Identification code	TPSI I	
Empirical formula	C_{24} H_{23} I N_2	
Formula weight	466.34	
Temperature	100(2) K	
Wavelength	0.71073 Å	
Crystal system	Triclinic	
Space group	$P\bar{1}$	
Unit cell dimensions	a = 11.2655(13) Å	α= 87.413(6)°.
	b = 13.6748(16) Å	β= 74.285(5)°.

	c = 15.7542(19) Å	γ = 66.856(6)°.
Volume	2143.1(4) Å3	
Z	4	
Density (calculated)	1.445 Mg/m3	
Absorption coefficient	1.504 mm^{-1}	
F(000)	936	
Crystal size	0.579 x 0.446 x 0.365 mm3	
Theta range for data collection	2.036 to 33.321°.	
Index ranges	-17≤h≤17, -21≤k≤21, -24≤l≤24	
Reflections collected	40269	
Independent reflections	16359 [R(int) = 0.022]	
Completeness to theta = 25.242°	99.7 %	
Absorption correction	Semi-empirical from equivalents	
Max. and min. transmission	0.5658 and 0.5139	
Refinement method	Full-matrix least-squares on F^2	
Data / restraints / parameters	16359 / 0 / 507	
Goodness-of-fit on F^2	1.033	
Final R indices [I>2sigma(I)]	R1 = 0.0328, wR2 = 0.0838	
R indices (all data)	R1 = 0.0531, wR2 = 0.0939	
Largest diff. peak and hole	0.651 and -0.389 e.$Å^{-3}$	

Table S2.

Crystal data and structure refinement for TPSI PF_6.

Identification code	TPSI PF_6	
Empirical formula	C_{24} H_{23} F_6 N_2 P	
Formula weight	484.41	
Temperature	100(2) K	
Wavelength	0.71073 Å	
Crystal system	Triclinic	
Space group	P-1	
Unit cell dimensions	a = 7.7668(4) Å	α= 98.578(3)°.
	b = 9.7052(5) Å	β= 99.776(3)°.
	c = 15.0202(8) Å	γ= 90.498(3)°.
Volume	1102.60(10) Å3	
Z	2	
Density (calculated)	1.459 Mg/m3	
Absorption coefficient	0.190 mm^{-1}	
F(000)	500	

Crystal size	0.514 x 0.239 x 0.142 mm3
Theta range for data collection	2.123 to 36.338°.
Index ranges	-12≤h≤12, -15≤k≤16, -25≤l≤23
Reflections collected	24286
Independent reflections	9455 [R(int) = 0.0319]
Completeness to theta = 25.242°	99.5 %
Absorption correction	Semi-empirical from equivalents
Max. and min. transmission	0.9282 and 0.8810
Refinement method	Full-matrix least-squares on F^2
Data / restraints / parameters	9455 / 81 / 301
Goodness-of-fit on F^2	1.023
Final R indices [I>2sigma(I)]	R1 = 0.0506, wR2 = 0.1221
R indices (all data)	R1 = 0.0772, wR2 = 0.1383
Largest diff. peak and hole	0.860 and -0.559 e.Å^{-3}

.

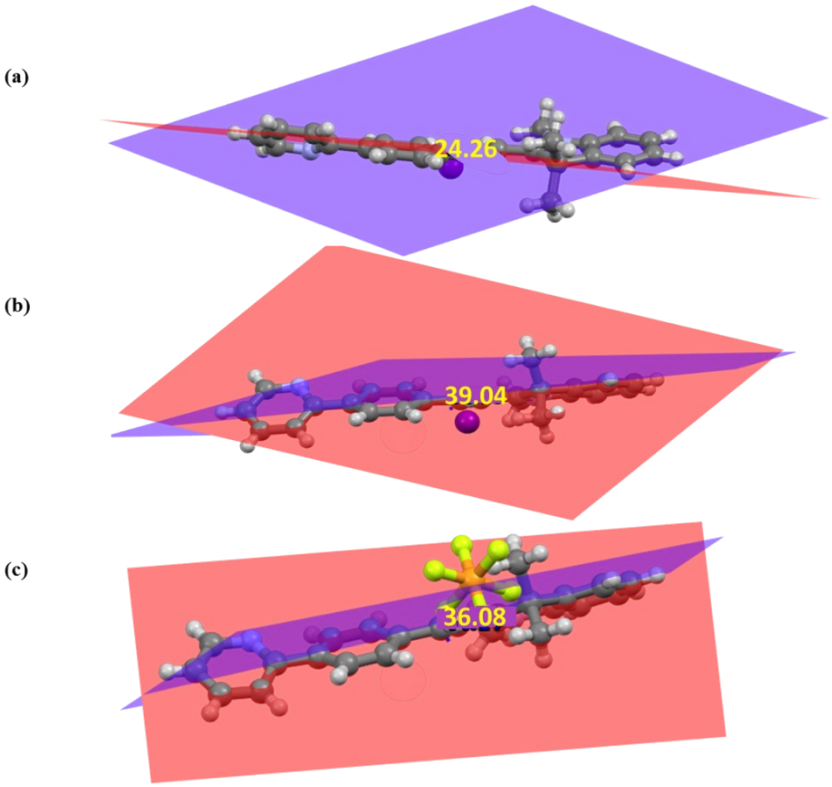

Figure S4. It shows the dihedral angle between the plane passing through the cyanine ring and phenyl pyridine ring (c, d) TPSI I and (e) TPSI PF_6 (Bluecolor plane = Plane passing through cyanine ring and Red color plane = Plane passing through the phenyl pyridine.)

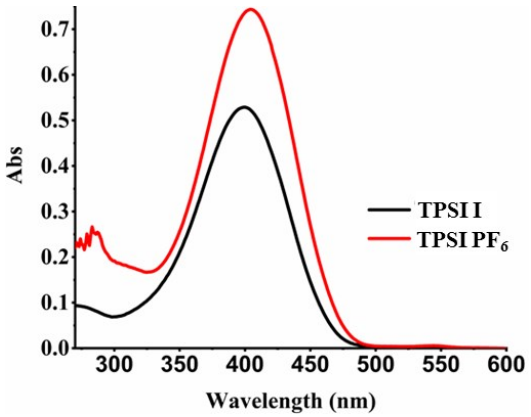

Figure S5. Absorption spectra of TPSI I and TPSI PF_6 in methanol ($1*10^{-5}$ M)

Electronic structure calculations.

Molecular structures were confirmed to be true minima on the ground state potential energy surface on the basis of their real harmonic vibrational frequencies. Methanol solvent effects were taken into account by the polarized continuum model with the integral equation formalism (IEFPCM)[2-3], and transition energies in solution were obtained with the linear response approach[4-5]. Wave function-based methods were also used to further evaluate interstate relative energies and the nature of electronic states. Additional multiconfigurational calculations were performed in order to confirm the shrinkage of the S_o/S_1gapupon molecular torsion. Concretely, the restricted active space configuration interaction spin-flip (RASCI-SF or RAS-SF) method within the hole and electron approximation[6] has been employed. The lowest triplet and quintet configurations of $TPSI^+$ were used as the reference. In order to ensure the robustness of the results, calculations were done with different number of active orbitals and electrons in the RAS2 orbital space. The RAS1 and RAS_3 spaces included all occupied and virtual orbitals, respectively. RAS-SF calculations were performed with the 6-31G(d) basis set. In order to characterize computed states, the number of unpaired electrons (N_U) was computed as indicated .[7]

IR simulated spectrum

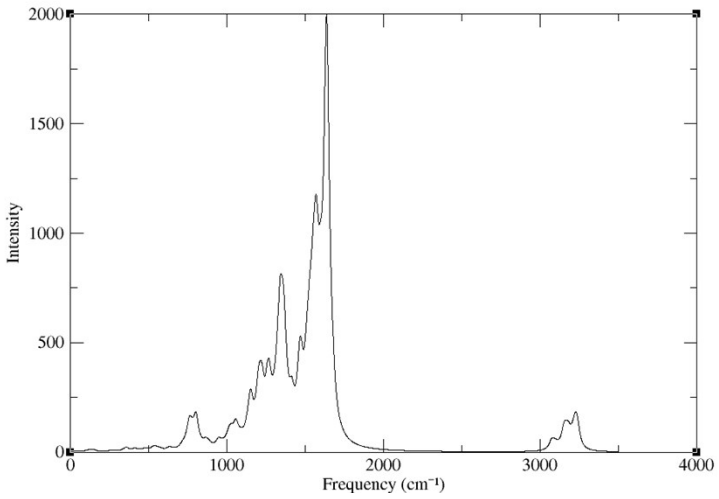

Figure S6. Simulation of the IR spectrum of $TPSI^+$ computed at the B3LYP/6-31G(d) level in methanol solution.

UV-vis simulated spectrum

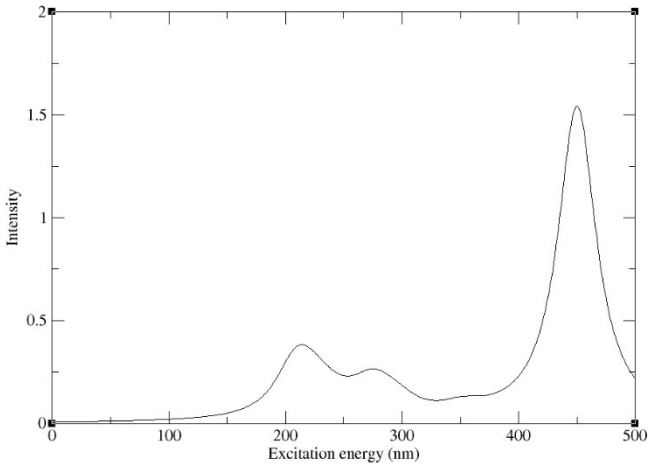

Figure S7. Simulation of the UV-vis absorption spectrum of $TPSI^+$ computed at the B3LYP/6-31G(d) level in methanol solution.

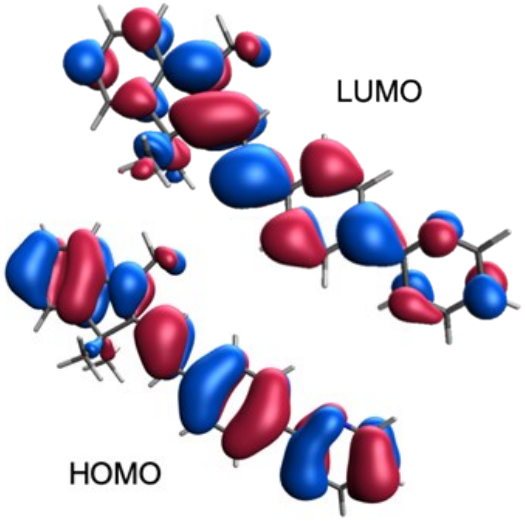

Figure S8.Frontier molecular orbitals (HOMO and LUMO) of $TPSI^+$computed at the B3LYP/6-31G(d) level

Table S3. Vertical excitation energies (ΔE*in* eV), oscillator strengths and main orbital contribution to the lowest singlet and triplet states of $TPSI^+$ in methanol solution computed with the B3LYP functional and the 6-31G(d) basis set.

state	ΔE	strength	composition
T_1	1.75	-	H→L
T_2	2.68	-	H-1→L
T_3	3.06	-	H-4→L
T_4	3.28	-	H-3→L

T_5	3.33	-	H-2→L
T_6	3.46	-	H-5→L
T_7	3.65	-	H→L+1
T_8	3.94	-	H-3→L+3
T_9	4.06	-	H-6→L
T_{10}	4.14	-	H→L+2

S_1	2.76	1.535	H→L
S_2	3.42	0.002	H-2→L
S_3	3.44	0.008	H-1→L
S_4	3.53	0.027	H-3→L
S_5	3.57	0.008	H-4→L
S_6	4.17	0.051	H-5→L
S_7	4.40	0.092	H-6→L
S_8	4.60	0.091	H→L+1
S_9	4.88	0.002	H-2→L+1
S_{10}	4.90	0.004	H→L+2

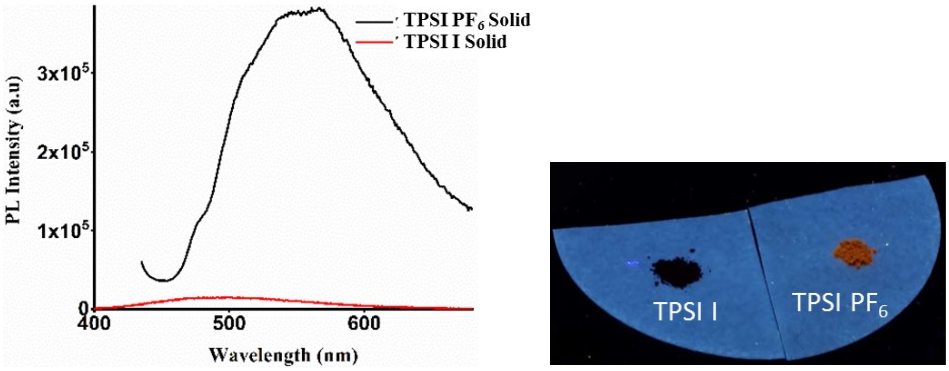

(a) (b)

Figure S9. (a) Emission spectra of TPSI I and TPSI PF_6 in solid state(b) Showing photoluminescence image of TPSI I and TPSI PF_6 in solid powdered form.

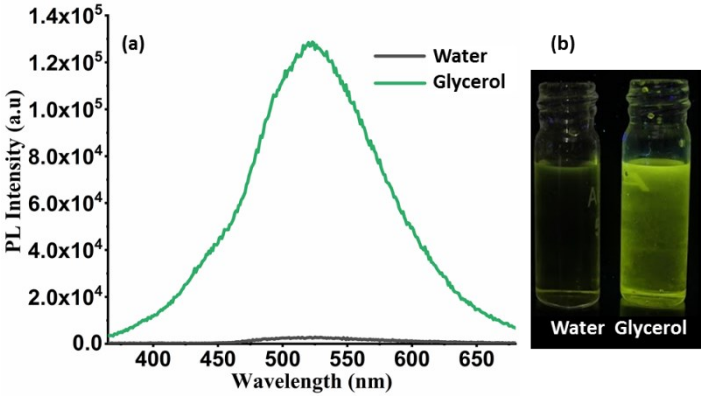

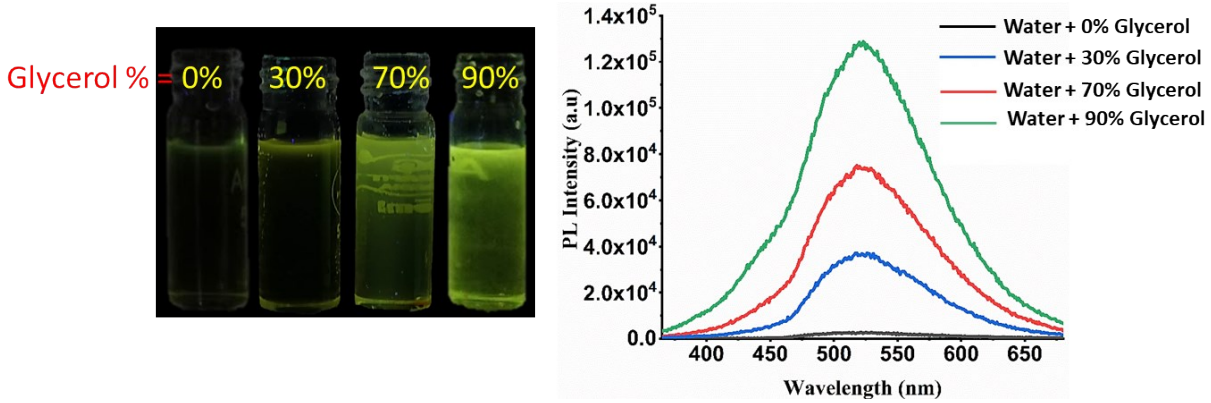

(c) (d)

Figure S10(a) Emission spectra of TPSI I in presence of water (1cP) and glycerol (1412cp) (C = 0.12 mM) (b) Photoluminescence image of TPSI I in presence of water and glycerol under 365 nm UV lamp. (c) Photoluminescence image of TPSI I ($1x10^{-5}$ M) in presence of different concentrations of glycerol (d) Emission spectra of TPSI I ($1x10^{-5}$ M) in presence of different concentrations of glycerol

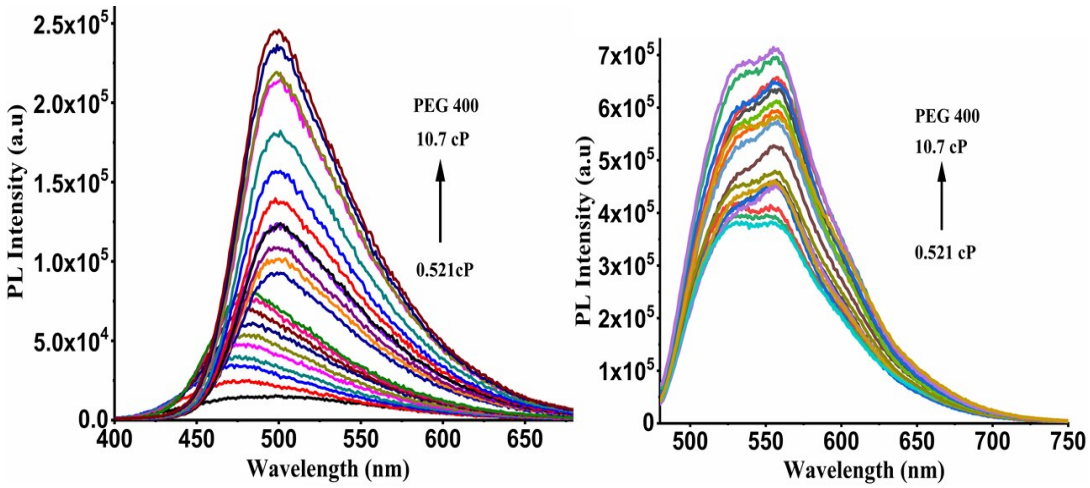

(a) **(b)**

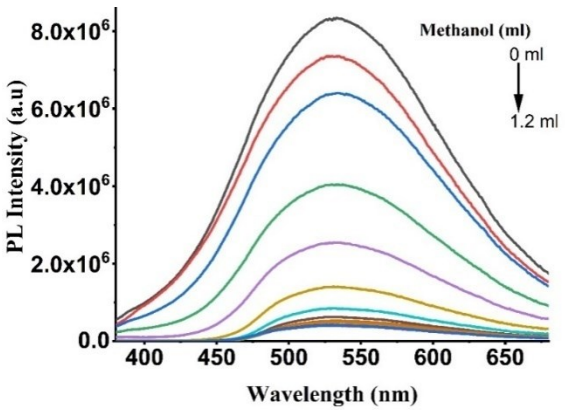

(c)

Figure S11. Emission spectra of (a) TPSI I and (b) TPSI PF_6 in methanol (C = $1*10^{-5}$ M) with gradually increasing the viscosity by adding PEG 400 (λ_{ext} = 365 nm)(c) Emission spectra of TPSI I ($1*10^{-5}$ M) with gradually increasing the methanol in PEG400 solution; the PL intensity is gradually decreasing with increasing concentration of methanol into PEG.(λ_{ext} = 365 nm)

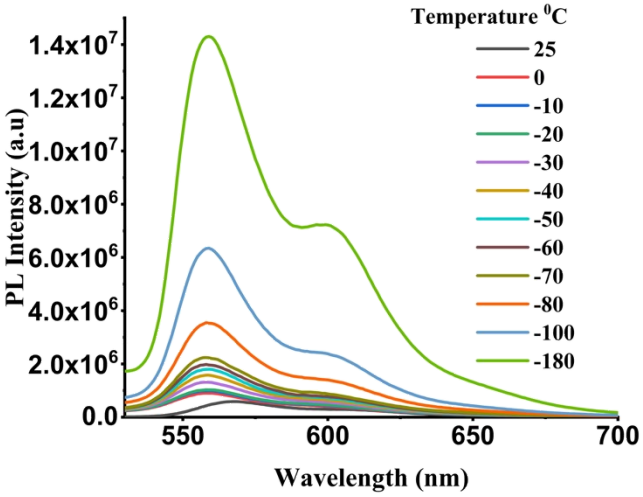

Figure S12. Emission spectra of TPSI I (in methanol C = $1*10^{-5}$ M) with gradually decreasing the temperature (λ_{ext} = 520 nm).

Table S4. Relative energies between the triplet and two lowest singlet states (ΔE in eV) of $TPSI^+$ at 90° of molecular torsion computed in vacuum at the RAS-SF/6-31G(d) level with 4 (6) electrons in 4 (6) orbitals in the RAS2 spaces and the Hartree-Fock triplet as the reference configurations. N_U = number of unpaired electrons.

	RAS(4,4)-SF		RAS(6,6)-SF	
state	ΔE	N_U	ΔE	N_U
T_1	0.00	2.04	0.00	2.05
S_0	0.05	1.93	0.05	1.91
S_1	0.38	0.18	0.29	0.22

Table S5. Relative energies between the triplet and two lowest singlet states (ΔE in eV) of $TPSI^+$ at 90° of molecular torsion computed in vacuum at the RAS-SF/6-31G(d) level with 4 (6 and 8) electrons in 4 (6 and 8) orbitals in the RAS2 spaces and the Hartree-Fockquintet as the reference configurations. N_U = number of unpaired electrons.

	RAS(4,4)-SF		RAS(6,6)-SF		RAS(8,8)-SF	
state	ΔE	N_U	ΔE	N_U	ΔE	N_U
T_1	0.00	2.11	0.00	2.17	0.00	2.26
S_0	0.06	2.05	0.05	2.09	0.05	2.15

S_1	1.01	0.16	0.53	0.34	0.51	0.43

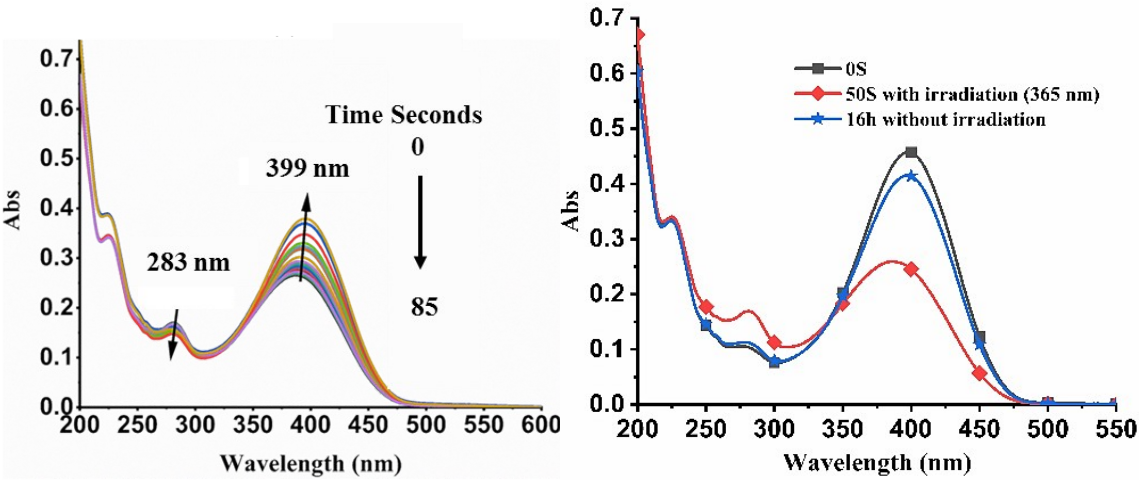

(a) (b)

Figure S13. (a) UV-Visible absorption spectra of TPSI PF_6 in methanol ($1*10^{-5}$ M) without irradiation with respect to time. (b) Reversible nature of the TPSI I shown before and after irradiation.

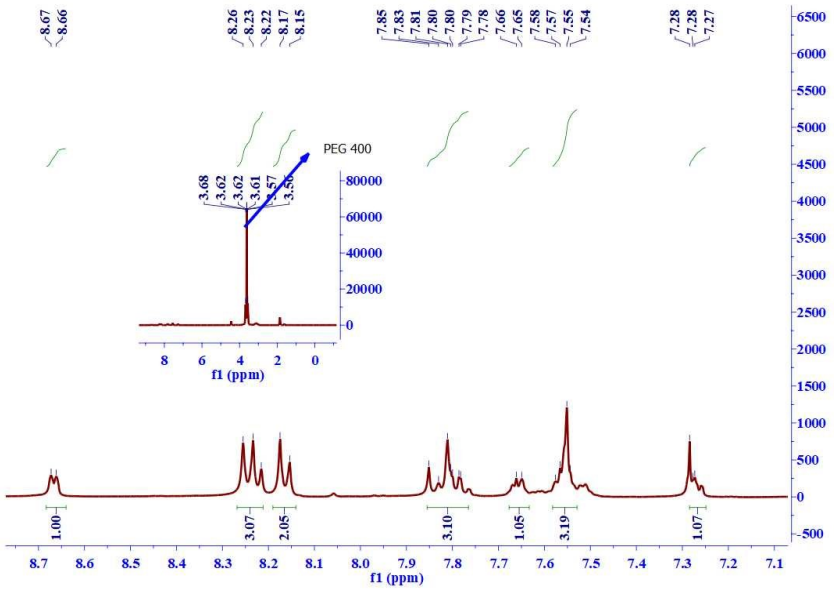

(a)

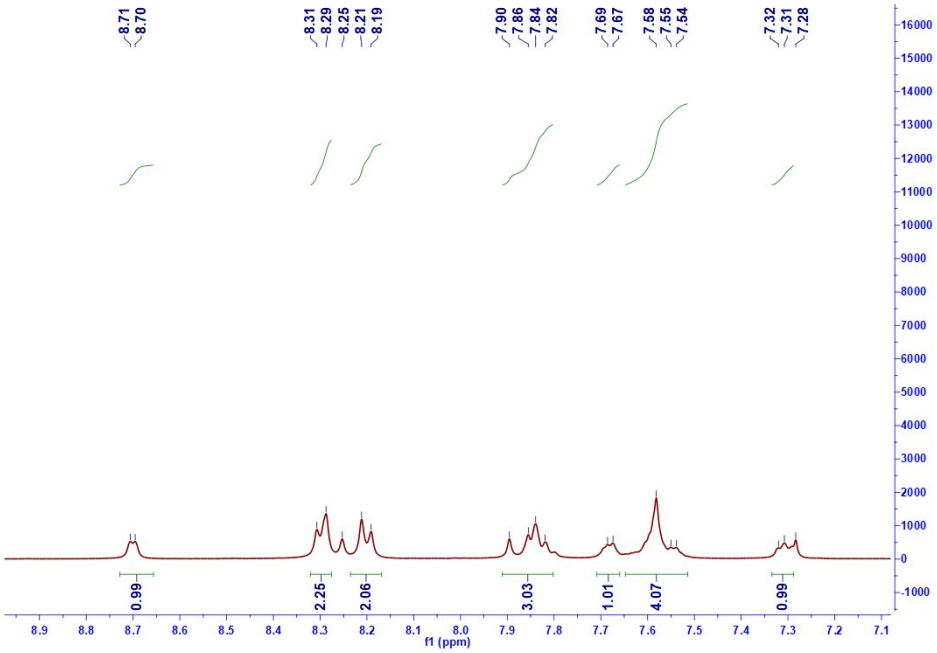

(b)

Figure S14. (a) ^{1}H NMR spectrum of TPSI I in presence of 1 equivalent of PEG 400;(b) ^{1}H NMR spectrum of TPSI I without PEG-400

Crystal structure and discussion

(a)

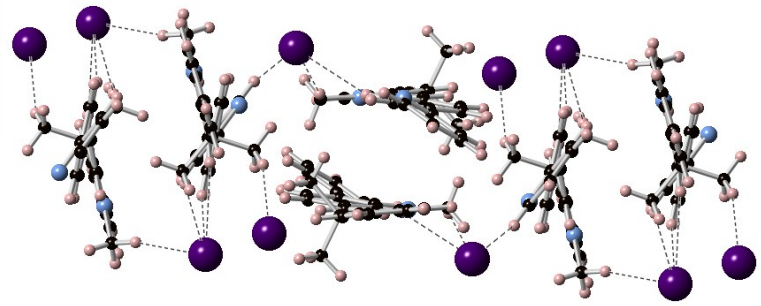

(b)

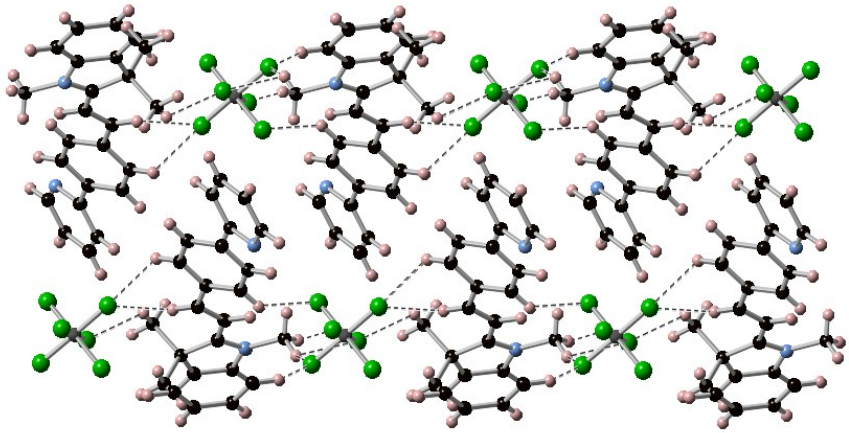

Figure S15. Crystal packing of $TPSI^+$ cations in TPSI I and TPSI PF_6, showing the arrangement into dimers leaving a considerable empty space within these dimers for TPSI I(a) and a compact packing of individual cations and anions in the case of TPSI PF_6 (b).

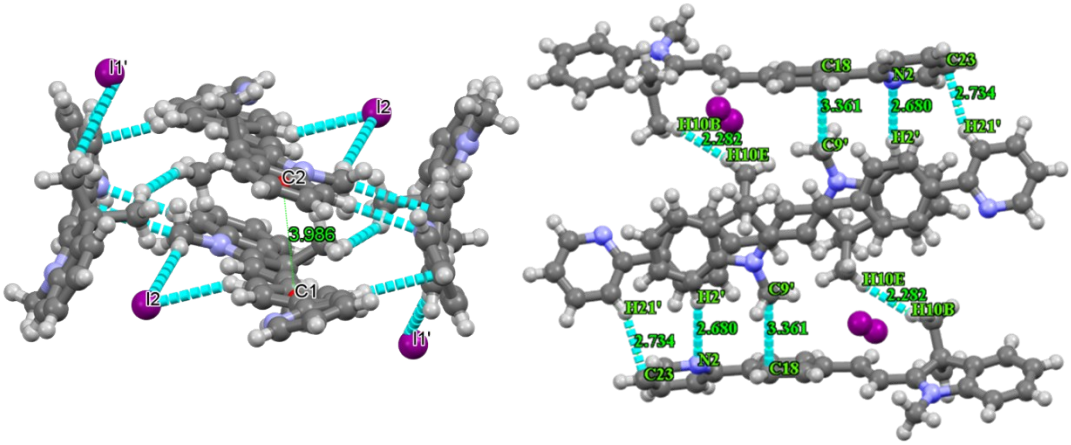

(a) (b)

Figure S16. Unit Cell of TPSI I showing that the distance between the two centroids (C1-C2) is 3.99 Å (c). Rest of the short contacts between the molecules, apart from short-contacts containing iodide (N2---H2' - 2.680 Å, C23---H21'-2.734 Å, C18---C9-3.361 Å and H10E----H10B-2.282 Å) (d).

In the TPSI I dimer, the six-membered carbon rings on the cyanine ring in one molecule and the phenyl ring in the other one are practically superposed (Fig. S16(a), ESI†), although the distance between the two centroids, 3.99 Å, is definitely beyond the range of distances for typical π-π interactions (3.3 – 3.9 Å). Each iodide anion is involved in several H-bond interactions with different cations in the unit cell: I1 with H15 (3.051 Å) and H11B (3.083 Å); I2 and I2' with H19' (3.008Å) and H9'B (3.140Å); and I1' with H11B' (3.284 Å) and H15' (3.110 Å). The shortest of these contacts are shown in Fig. 2a (I···H < 3.1 Å). Other than the $TPSI^+$··· I^- interactions, there are four more short contacts between two side-by-side molecules in the unit cell: one between the nitrogen of phenyl pyridine (N2) and the hydrogen (H2') on the phenyl ring in the cyanine fragment (N2---H2' -, 2.680 Å), another between C23 of the pyridine ring with (H21') of the pyridine ring of the second molecule (C23---H21', 2.734 Å), the third one between C18 of phenyl ring with C9 of cyanine ring (C18---C9-, 3.361 Å), and a fourth hydrogen-hydrogen bond interaction between dimethyl group on cyanine ring (H10E---H10B-2.282 Å)(Fig. S16(b), ESI†). In this unit cell, each PF_6^- anion is involved in three interactions in the form of hydrogen bonds with the TPSI+ cations which are: F3---H15 (2.462 Å), F3----H13 (2.596 Å) and F2----H10B (2.598Å) (Fig. 2b).

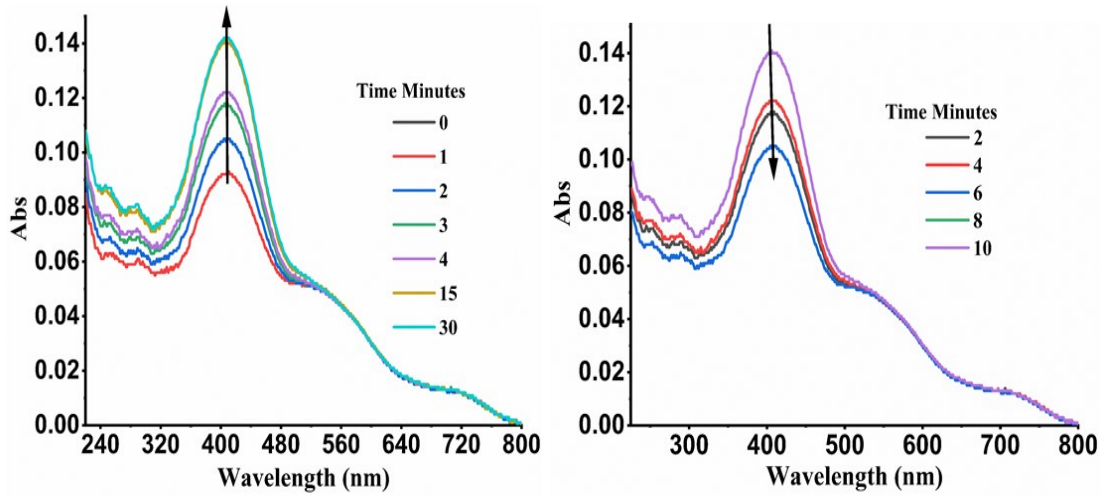

(a) (b)

Figure S17. (a) UV-Vis spectra of TPSI I solid state on irradiation at 365 nm as a function of time (b) UV-Visible spectra of TPSI I solid staterecorded by switching off UV-the lamp

Table S6. Relative ground state energies (in kcal/mol), and adiabatic (with respect to the ground state minimum) and vertical excitation energies to the lowest excited singlet S1 (in eV) along the molecular torsion (in degrees) of the central C=C double bond of $TPSI^{+}$computed at the B3LYP/6-31G(d) level. Molecular geometries have been optimized for the ground state at each torsion angle. Ground state minimal energy *cis* and *trans* conformations highlighted in grey.

tor.	$E(S_o)$	$\Delta E_{ad}(S_1)$	$\Delta E_v(S_1)$
40	20.43	3.32	2.43
50	22.47	3.33	2.35
60	16.98	3.35	2.61
90	27.96	3.44	2.23
120	42.80	3.06	1.20
150	3.74	2.86	2.70
180	0.00	2.75	2.75

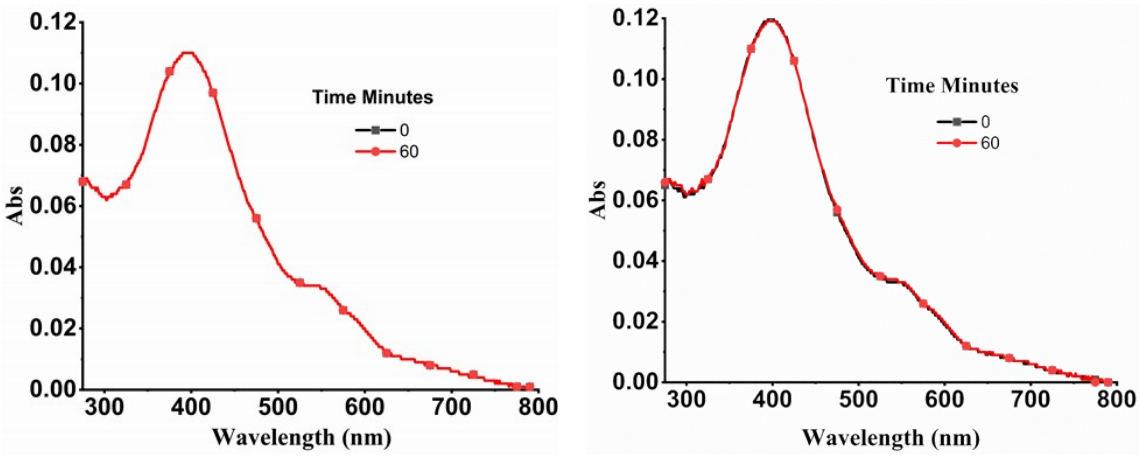

Figure S18. (a) UV–vis spectral changes of TPSI PF_6 in solid state (powder form) upon irradiation at 250 nm as a function of time (b) UV-Vis spectra of TPSI PF_6 on irradiation at 365 nm as a function of time

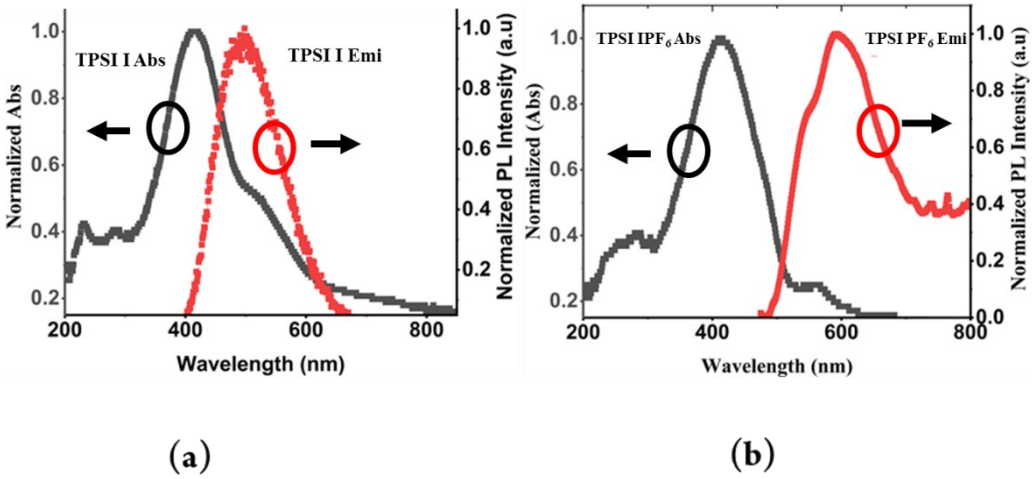

Figure S19. Overlapped Spectra of (a) TPSI I and (b) TPSI PF_6 absorption and emission in the solid state.(Overlapped intergra J(λ) for TPSI I = 3.46 x10^{16} and TPSI PF_6 = 1.912 x10^{13})

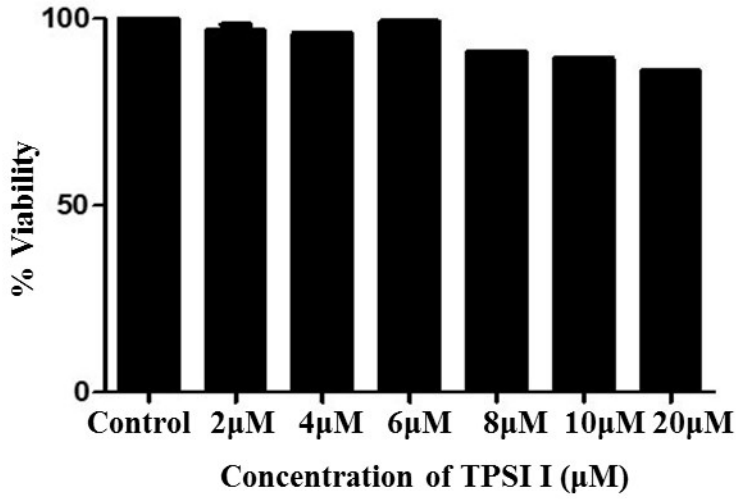

Figure S20 Dose kinetics study of TPSI I in Huh7 cells for viability was performed to understand any cytotoxic effect imparted by the compound on the tumor cells

Optimized geometry of $TPSI^{+}$

Cartesian coordinates in Angstroms.

C	72.704038	14.440614	4.084793
C	73.808900	14.296219	4.918605
C	71.180381	13.573385	1.090484
C	71.251033	16.113491	1.430973
C	69.131573	14.592386	3.453941
C	68.266519	14.744057	2.405584
C	66.821837	14.741162	2.470323
C	66.099437	14.895803	1.267341
C	64.711854	14.892055	1.256089
C	63.984774	14.733063	2.449276
C	64.703360	14.591824	3.654962
C	66.087085	14.591765	3.669134
C	62.499059	14.717423	2.470872
C	61.739960	14.465842	1.316144
C	60.349737	14.467868	1.403189
C	59.750552	14.714981	2.636864
C	60.583114	14.941621	3.735397
C	75.067373	14.328289	4.310988
C	75.199192	14.496729	2.927909
C	74.070293	14.636143	2.111013

C	72.814652	14.605647	2.703414
C	71.428824	14.724513	2.098378
C	70.550250	14.588891	3.347266
C	70.837682	14.309579	5.803347
H	71.288939	12.597459	1.572501
H	71.916386	13.641640	0.283925
H	70.184898	13.630659	0.644331
H	70.255453	16.231181	0.996934
H	71.985837	16.218544	0.627401
H	71.413383	16.920169	2.151668
H	68.723737	14.453965	4.448484
H	68.669432	14.879005	1.407877
H	66.640998	15.025161	0.334351
H	64.196586	15.035119	0.312565
H	64.147893	14.478581	4.578442
H	66.600835	14.472453	4.617467
H	73.719654	14.159257	5.990055
H	62.221691	14.252024	0.368842
H	59.747070	14.272532	0.521165
H	58.671652	14.726409	2.752312
H	60.154732	15.131312	4.718063
H	75.954098	14.218452	4.927253
H	76.188764	14.517521	2.482076
H	74.181593	14.762774	1.038241
H	70.345776	13.342363	5.931651
H	70.140656	15.117265	6.031595
H	71.681931	14.376383	6.484864
N	71.324424	14.447968	4.426007
N	61.916740	14.944306	3.666973

References

(1) Lohitesh, K.; Saini, H.; Srivastava, A.; Mukherjee, S.; Roy, A.; Chowdhury, R., Autophagy inhibition potentiates SAHA-mediated apoptosis in glioblastoma cells by accumulation of damaged mitochondria. *Oncol. Rep.* **2018,***39* (6), 2787-2796.
(2) Cancès, E.; Mennucci, B., Comment on "Reaction field treatment of charge penetration" [J. Chem. Phys. 112, 5558 (2000)]. **2001,***114* (10), 4744-4745.
(3) Chipman, D. M., Reaction field treatment of charge penetration. *J. Chem. Phys.* **2000,***112* (13), 5558-5565.

(4) Cammi, R.; Mennucci, B., Linear response theory for the polarizable continuum model. *J. Chem. Phys.* **1999,***110* (20), 9877-9886.
(5) Cossi, M.; Rega, N.; Scalmani, G.; Barone, V., Polarizable dielectric model of solvation with inclusion of charge penetration effects. *J. Chem. Phys.* **2001,***114* (13), 5691-5701.
(6) Casanova, D.; Head-Gordon, M., Restricted active space spin-flip configuration interaction approach: theory, implementation and examples. *Phys. Chem. Chem. Phys.* **2009,***11* (42), 9779-9790.
(7) Head-Gordon, M., Characterizing unpaired electrons from the one-particle density matrix. *Chem. Phys. Lett.* **2003,***372* (3), 508-511.